27. O. Torres, P. K. Bhartia, *J. Geophys. Res.* **104**, 21569 (1999).
28. Additional maps illustrating the regional TTO increase in March 1997 are at http://metosrv2.umd.edu/~tropo. Animation of superimposed TTO and smoke aerosol from July through October 1997 is available on *Science* Online at www.sciencemag.org/cgi/content/full/291/5511/2128/DC1. The March ozone jump also coincided with a satellite-based upper-tropospheric H_2O decrease (*29*). Unfortunately, there are no H_2O data in the Watukosek soundings to verify the H_2O-ozone relation.
29. S. Chandra, J. R. Ziemke, W. Min, W. G. Read, *Geophys. Res. Lett.* **25**, 3867 (1998).
30. The SOI is defined as a normalized difference of sea-level pressure anomalies between the eastern Pacific (Tahiti) and the Maritime Continent (Darwin). The DMI (Fig. 1B) is an index of the IOD (*31*) that estimates anomalous fluctuations of the equatorial sea-surface temperature (SST) gradient in the Indian Ocean. In the time period of this analysis, ENSO and IOD, two independent phenomena, occur simultaneously. As SST conditions change, there are variations in convection and subsidence (downward motion, negative SOI, and increase in TTO). Outgoing longwave radiation (OLR) is used here as a proxy for deep convection, a positive OLR anomaly signifying less convective activity or rainfall than usual and, consequently, anomalous subsidence. Early March marked the start of an ENSO/IOD event (SOI-negative, DMI-positive, OLR-positive) that reached greatest instensity by October 1997, coincident with maximum TTO. Downward mixing by an equatorial Kelvin wave and the Madden-Julian Oscillation may also enhance TTO over Indonesia during the 1997 fires (*19*).
31. N. H. Saji, B. N. Goswami, P. N. Vinayachandran, T. Yamagata, *Nature* **401**, 360 (1999).
32. Typical ozone-formation rates in savanna-burning regions, 10 to 15 parts per billion by volume of ozone/day in the boundary layer (*5, 9, 10*), are equivalent to 2 to 4 DU/day. Although ozone is destroyed at the surface, it may form above the boundary layer after convective transport of ozone precursors. Free tropospheric ozone–formation rates are lower, but ozone persists for several weeks or more (*5, 9*) and keeps forming as ozone precursors are transported downwind. This is referred to as "mix-then-cook" by Chatfield and Delany (*33*). Alternatively, if ozone formed near the surface is mixed up to the free troposphere, "cook-then-mix" (*33*), it can accumulate in recirculating air parcels. Recirculation may have contributed to high TTO (70 DU) over Indonesia—50 to 60 DU is a typical value over African burning (*7*). On the other hand, ozone photochemical formation over Indonesia may have been greater than over African savanna fires because smoldering combustion near Kalimantan peat bogs produced ozone precursors at a higher rate (*34*). Sampling on a commercial airliner recorded elevated CO concentrations at 8 to 13 km over Indonesia after mid-September 1997. This implies exhalation of the lower troposphere.
33. R. B. Chatfield, A. D. Delany, *J. Geophys. Res.* **95**, 18473 (1990).
34. H. Matsueda, H. Y. Inoue, *Geophys. Res. Lett.* **24**, 2413 (1999).
35. K. Kita, M. Fujiwara, S. Kawakami, *Atmos. Environ.* **34**, 2681 (2000).
36. Y. Tsutsumi *et al.*, *Geophys. Res. Lett.* **26**, 595 (1999).
37. The model used is the isentropic trajectory model of M. R. Schoeberl and P. A. Newman [*J. Geophys. Res.* **100**, 25801 (1995)]. Clusters of trajectories are initialized at the 310 K potential temperature level for the smoke and at 316 and 331 K for the ozone layers. Winds are taken from National Center for Environmental Prediction (NCEP) 2.5° by 2.5° analysis.
38. J. P. Burrows *et al.*, *J. Atmos. Sci.* **56**, 155 (1999). GOME also detected elevated carbon monoxide and formaldehyde.
39. The statistical method used in Figs. 4 and 5 is based on the method described by S. M. Hollandsworth *et al.* [*Geophys. Res. Lett.* **22**, 905 (1995)]. The Nimbus 7 record covers 14 full years, but the start-up year is omitted and 1991–1992 data are not used because of aerosol artifacts after the Mount Pinatubo, Philippines, eruption. No tropical regions displayed a tropospheric ozone trend in the 1980s, according to the modified-residual method (*7*). An alternate technique for deriving TTO from TOMS (*40*) also shows no statistically significant ozone trend in the 1980s. See TTO during the 1982–1983 ENSO at http://metosrv2.umd.edu/~tropo.
40. S. Chandra, J. R. Ziemke, R. W. Stewart, *Geophys. Res. Lett.* **26**, 185 (1999).
41. J. F. Gleason, N. C. Hsu, O. Torres, *J. Geophys. Res.* **103**, 31969 (1998).
42. N. C. Hsu *et al.*, *J. Geophys. Res.* **104**, 6269 (1999).
43. R. D. Hudson, A. D. Frolov, in preparation.
44. There appears to be a trend in total ozone when TOMS data are analyzed by latitude band, but the trend in tropical total ozone disappears when analysis is done within a meteorologically coherent regime (*43*). The lack of a TTO trend (*7*) is not surprising because the modified-residual method is restricted to a meteorologically defined tropical band (*25*).
45. In January 1993 and January 1999, during northern African biomass burning, the highest ozone over the Atlantic was observed south of the Intertropical Convergence Zone (*11, 12*) a phenomenon designated the "tropical Atlantic paradox." According to Moxim and Levy (*14*), lightning is the dominant tropical NO source except during the southern African burning season.
46. We are grateful to the TOMS Ozone Processing Team for real-time data; S. M. Hollandsworth, T. L. Kucsera, and M. G. Seybold (Science Systems and Applications at NASA-Goddard) for assistance with the regression model; and A. D. Frolov and A. K. Kochhar for work on the University of Maryland Web site. H. Saji generously provided the OLR and DMI. Comments on the manuscript by R. B. Chatfield, J. F. Gleason, R. S. Stolarski, J. P. Burrows, and A. Ladstätter-Weißmayer are greatly appreciated. Supported by NASA Programs in Atmospheric Chemistry, Modeling and Analysis (ACMAP) and Tropospheric Chemistry.

24 October 2000; accepted 13 February 2001

Synchronous Tropical South China Sea SST Change and Greenland Warming During Deglaciation

M. Kienast,[1]* S. Steinke,[2] K. Stattegger,[2] S. E. Calvert[1]

The tropical ocean plays a major role in global climate. It is therefore crucial to establish the precise phase between tropical and high-latitude climate variability during past abrupt climate events in order to gain insight into the mechanisms of global climate change. Here we present alkenone sea surface temperature (SST) records from the tropical South China Sea that show an abrupt temperature increase of at least 1°C at the end of the last glacial period. Within the recognized dating uncertainties, this SST increase is synchronous with the Bølling warming observed at 14.6 thousand years ago in the Greenland Ice Sheet Project 2 ice core.

Previous studies of the phase relation between tropical and high-latitude warming during the last deglaciation came to contrasting conclusions: the tropical ocean was either synchronous with (*1*) or led (*2, 3*) the Northern Hemisphere deglacial temperature increase. Antiphasing between changes in tropical Atlantic SST and temperature over Greenland is expected based on the bipolar see-saw mechanism (*4*). But the timing of deglacial SST increases in the Pacific and Indian Oceans relative to high-latitude warming is still controversial. On the basis of a radiocarbon-dated alkenone thermometry (U^K_{37})-SST record from the tropical northwestern Indian Ocean, Bard *et al.* (*1*) inferred an interhemispheric synchrony of deglacial warming in the Arabian Sea and Greenland, specifically during the Bølling Transition at the end of the last glaciation. However, this Indian Ocean U^K_{37}-SST change leads planktonic foraminiferal $\delta^{18}O$ from the same core (*5*) during this abrupt event. A similar lead of foraminiferal Mg/Ca-derived SST estimates versus $\delta^{18}O$, as well as the correspondence between equatorial Pacific foraminiferal Mg/Ca and Antarctic temperature records, however, prompted Lea *et al.* (*2*) to postulate a lead of tropical Pacific deglacial SST increase versus ice volume, and a synchroneity with Antarctic warming during deglaciation.

Here we present two high-resolution, accelerated mass spectrometry (AMS) ^{14}C-dated U^K_{37}-SST and foraminiferal $\delta^{18}O$ records (Fig. 1, A and B) (*6*) from the tropical southern South China Sea (SCS), a non-upwelling environment within the Western Pacific Warm Pool (WPWP), that cover the late glacial–to-Holocene transition. Sediment cores 18252-3 and 18287-3 were retrieved from the southwestern (9°14′N, 109°23′E, 1273-m water depth) and southern (5°39′N, 110°39′E, 598-m water depth) SCS, respectively. According

[1]Earth and Ocean Sciences, University of British Columbia, Vancouver, B.C. Canada V6T 1Z4. [2]Institut für Geowissenschaften, Universität Kiel, Kiel, Germany.

*To whom correspondence should be addressed. E-mail: kienast@unixg.ubc.ca

to the radiocarbon chronologies, both cores have sedimentation rates of 20 to >60 cm/thousand years (cm/ka). Core 18287-3 contains an undisturbed hemipelagic sequence, whereas core 18252-3 contains several small turbidites (1 to 5 cm thickness) in the lower part of the core (Fig. 1A) (*7*) that are readily identified macroscopically and by bulk sediment geochemistry (*8*).

The late glacial parts of the two downcore records show low SSTs of about 25.2°C and 25.9°C in cores 18252-3 and 18287-3, respectively, and high planktonic $\delta^{18}O$ values (about –1.5‰). In contrast, the Holocene displays warm temperatures of 26.5° to 28.0°C and 27.2° to 28.3°C in cores 18252-3 and 18287-3, respectively, and low $\delta^{18}O$ values of about –3.1‰ (Fig. 1, A and B). The SST difference between the late glacial and the Holocene of up to 3°C agrees with previous U^{K}_{37}-SST records from the southern SCS (*9*) and corroborates the growing body of evidence from alkenone (*1*, *3*, *9*) and foraminiferal Mg/Ca (*2*, *10*) paleothermometry for a tropical glacial cooling of ~3°C. In both records, planktonic $\delta^{18}O$ and U^{K}_{37}-SST estimates vary in concert during the transition from the late glacial to the Holocene, including much of the high-resolution, small-scale variability (Fig. 1, A and B). The most prominent event in both records is the abrupt warming of at least 1°C at 385 to 405 cm in core 18252-3, and at 435 to 450 cm in core 18287-3 (Fig. 1, A and B).

The $\delta^{18}O$ and U^{K}_{37}-SST trends at both SCS sites are interpreted to uniquely reflect changes in local sea surface conditions, unaffected by variations in, for example, riverine input, advection of different water masses, or upwelling. This assertion is based not only on the similarity of both records despite the different local setting of the core sites but is corroborated by planktonic foraminiferal census counts (core 18287-3; *11*), as well as organic $\delta^{13}C$ and inorganic (major/minor element composition) geochemical data from both cores (*8*) that do not show any significant variability associated with this particular warming event.

The abrupt deglacial warming event is the largest amplitude signal in SCS sedimentary records as well as the Greenland isotope record, and in both locations it is larger than the analytical error of the U^{K}_{37}-SST estimates and planktonic foraminiferal $\delta^{18}O$ determinations (*6*). The extreme rapidity of the event in the SCS is analogous to the Bølling Transition in the Greenland ice cores (Fig. 1C). Two independent lines of evidence, each of which has been used in previous studies to establish phasing relations between tropical and high-latitude climate, suggest synchroneity (referring to synchronous timing within the inevitable uncertainties of radiocarbon dating) of this warming in the SCS and at the Bølling Transition in Greenland. First, the midpoint of the abrupt warming in the southern SCS has interpolated AMS ^{14}C ages of 15,140/14,600/14,400 (core 18252-3) and 14,570 (core 18287-3) calibrated years (*12*). Thus, within the 1σ range of the calibrated AMS ^{14}C dates (*12*), these ages are identical with the age of the midpoint in the Greenland warming of 14,660 ± 300 years ago (*13*), as measured by the Greenland Ice Sheet Project 2 (GISP2). The ages of the midpoint of the warming event in both SCS cores are not interpolated over any major change in sedimentation rates as inferred from unchanged bulk sediment geochemistry (*8*) between the AMS ^{14}C control points. Moreover, the calibrated AMS ^{14}C ages have been derived assuming a minimal average oceanic resevoir age of –400 years

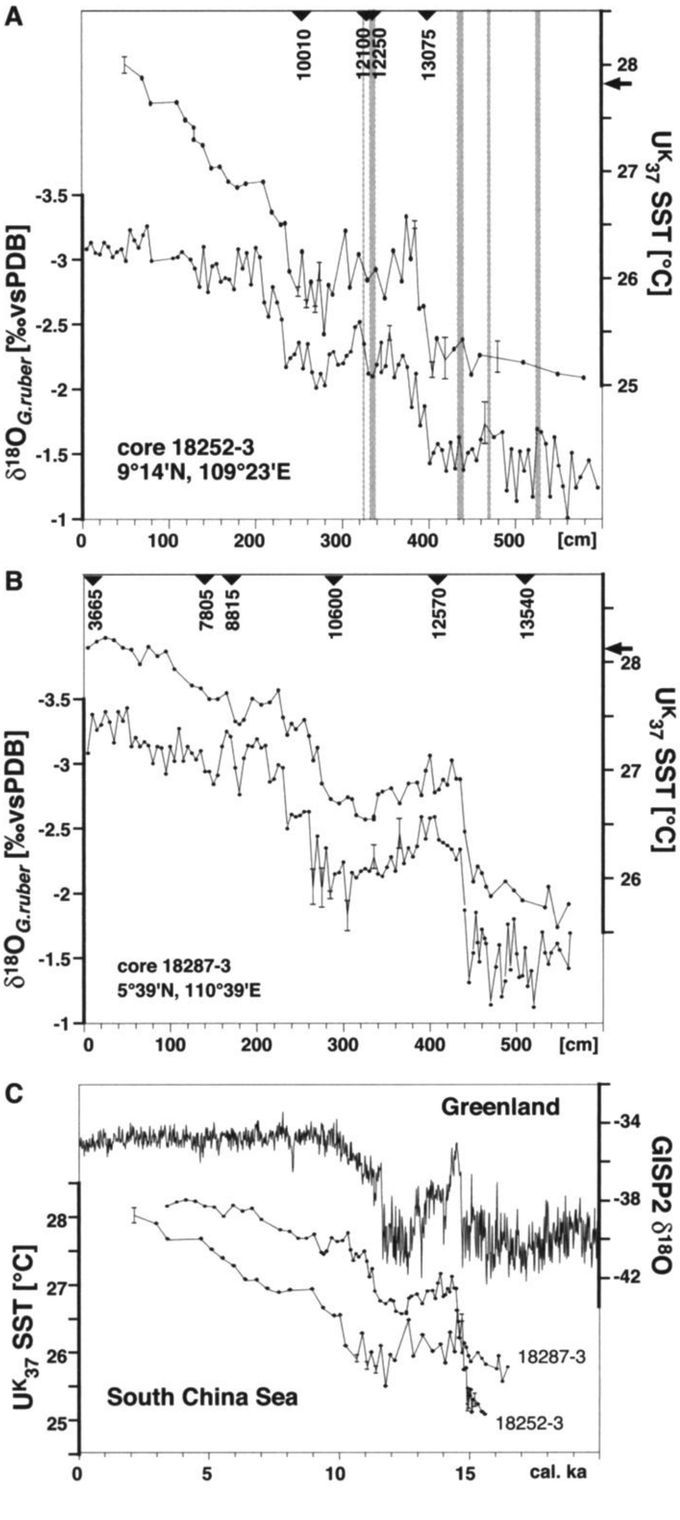

Fig. 1. Planktonic $\delta^{18}O$ and U^{K}_{37} SST estimates of core 18252-3 (**A**) and core 18287-3 (**B**) from the southern South China Sea versus core depth. Conventional AMS ^{14}C ages (bold numbers) are denoted by triangles on the upper x axes. Error bars show the SD of multiple isotope analyses and U^{K}_{37} SST estimates. Modern SST values at both sites are indicated by arrows on the y axes. The thin turbidites in core 18252-3 are indicated by vertical bars. All turbidites are considered instantaneous deposits. Thus, the radiocarbon age of 12,250 (335 cm) is assigned to the base of the turbidite at 333 to 338 cm for linear interpolation of the midpoint of the warming at 392.5 cm (*12*). Using the radiocarbon age of 12,100 (328 cm) between the two turbidites [(323 to 324 cm and 333 to 338 cm; see (A)] for linear interpolation yields identical ages for the midpoint of the warming. (**C**) U^{K}_{37}-SST records of cores 18252-3 and 18287-3 from the southern SCS on their independent calender time scales versus the GISP2 $\delta^{18}O$ record (*32*) on the time scale of (*13*). Note that the chronology of core 18252-3 less than 10,010 ^{14}C years is based on assigning an age of 0 years to the core top and linear interpolation in between, and thus should be considered tentative.

(*14*). Adopting a larger reservoir effect (*15*) would result in a lag of SCS versus Greenland warming rather than a lead. Second, based on the revised chronology of the deglacial rise in sea level from the southern SCS (*16*), the first major melt water pulse (MWP 1A) occurred at 14.6 to 14.3 thousand years ago (ka), synchronous (within dating uncertainties) with the Bølling Transition warming in Greenland. MWP 1A is associated with a decrease of $\delta^{18}O_{seawater}$ of up to ~0.2‰, which should also be reflected in a synchronous (*17*) step-like decrease of $\delta^{18}O_{G.ruber}$ (*6*). In both SCS cores, there is no indication for such a sustained decrease of $\delta^{18}O_{G.ruber}$ either preceding or postdating the abrupt increase in U^{K}_{37}-SSTs (Fig. 1, A and B). Thus, the $\delta^{18}O$ decrease related to MWP 1A most likely occurs synchronously with the temperature-related $\delta^{18}O_{G.ruber}$ decrease during the Bølling Transition in the SCS, thus increasing its amplitude slightly. This evidence also corroborates synchronous warming during the Bølling Transition in the southern SCS and Greenland. Accordingly, neither SCS core supports the idea that tropical SST increases led Greenland warming during the Bølling Transition. On the contrary, the records support earlier findings (*1*) from the northern Indian Ocean of synchronous deglacial warming in the tropics and high northern latitudes.

Previous records from the SCS displayed a similar parallelism between U^{K}_{37}-SST and $\delta^{18}O_{G.ruber}$ (*9*). There is, however, no radiocarbon age control for the abrupt deglacial warming in core 17964-3 (6°09′N, 112°13′E) from the southern SCS, and the midpoint of the abrupt warming in the northern SCS (core 17940-2; 20°07′N, 117°23′E) is radiocarbon dated at 15,970 years (*18*). This large difference in the radiocarbon age between the warming in northern (core 17940-2; *9*) and southern (this study) SCS is most likely due to a significantly higher reservoir age at the northern site, possibly caused by the advection of old Pacific intermediate- to deep-water masses (*15*).

The close parallelism between $\delta^{18}O_{G.ruber}$ and U^{K}_{37}-SSTs during the last deglaciation in the SCS contrasts markedly with the lead of U^{K}_{37}- and Mg/Ca-SST estimates over $\delta^{18}O_{G.ruber}$ in the Arabian Sea (*1, 19*), the equatorial Pacific (*2*), and the tropical Atlantic (*3, 10*). The variability of SST in the equatorial Pacific upwelling region during the last 250,000 years has previously been interpreted to reflect variable horizontal and/or vertical advection of different water masses (*20*), processes that are not likely to have affected the SCS given the secluded nature of the basin, particularly during glacial and early deglacial sea-level lowstands. Thus, equatorial open-ocean SST variability could be substantially influenced by changes in large-scale oceanic circulation patterns, which appear to show an early response to Southern Hemisphere deglaciation (*20, 21*), and may not affect the surface ocean in semi-enclosed marginal basins such as the SCS. The tropical SST records examined here suggest a diverse pattern of temporal changes in different parts of the tropical ocean during the glacial-interglacial transition.

Lastly, despite the very different temporal records of the onset of deglacial warming in various tropical marine records, there appears to be strong evidence that tropical Holocene SSTs increased steadily from ~10 to 6 ka, stabilizing thereafter (*1, 3, 9*, this study). In contrast, high-resolution mid- and high-northern latitude deglacial U^{K}_{37}-SST records (*22–25*) show an early Holocene SST optimum at ~10 to 9 ka. The establishment of maximum SSTs in the tropics after ~6 ka implies a stronger latitudinal SST contrast between ~10 and 6 ka, at the same time as an increased contrast in seasonal insolation evolved between the equator and high latitudes (*26*).

References and Notes

1. E. Bard, F. Rostek, C. Sonzogni, *Nature* **385**, 707 (1997).
2. D. W. Lea, D. K. Pak, H. J. Spero, *Science* **289**, 1719 (2000).
3. C. Rühlemann, S. Mulitza, P. J. Müller, G. Wefer, R. Zahn, *Nature* **402**, 511 (1999).
4. T. F. Stocker, *Quat. Res.* **19**, 301 (2000)
5. J. C. Duplessy *et al.*, *Earth Planet. Sci. Lett.* **103**, 27 (1991).
6. Planktonic foraminiferal $\delta^{18}O$ values (versus Pee Dee belemnite standard) were determined on 20 to 25 specimens of the surface-dwelling foraminifer *Globigerinoides ruber* (white) sensu stricto in the 250- to 400-μm size fraction at the Leibniz Laboratory in Kiel, Germany, with a 1σ analytical error of ±0.08‰. Alkenone determinations were carried out following procedures described in (*27*). Briefly, freeze-dried, manually ground sediment samples (7 to 11 g) were extracted with dichloromethane (ultrasonicated) and hydrolyzed with 6% KOH in methanol. The alkenones (and other neutral compounds) were separated from highly polar compounds using silica columns (20 cm by 0.5 cm) packed with 2 g of silica gel in a mixture of dichloromethane and n-hexane (8:2) and were eluted with 10 ml of the same solvent mixture. The final extracts were redissolved in toluene (20 μl final volume), and analyzed by gas chomatography (GC HP 5880A) at the University of British Columbia. The C_{37} alkenones were identified by their gas-chromatographic retention time by analogy with an extract of a pure *Emiliania huxleyi* culture. Selected samples were analyzed by GC–mass spectrometry (GC-MS) for confirmation of compound identification and evaluation of possible co-elutions. SST estimates were calculated with the use of an equation developed specifically for the SCS (*28*), $SST = (([C_{37:2}]/[C_{37:2}+C_{37:3}]) - 0.092)/0.031$, where $[C_{37:2}]$ and $[C_{37:3}]$ are concentrations of the di- and tri-unsaturated alkenones, respectively. This regional calibration yields slightly higher (by <0.3°C) SST estimates than the global calibration by Müller *et al.* (*29*); the amplitude of the deglacial SCS SST increase, however, remains the same. On the basis of multiple analyses of the same sediment extract as well as repeat extractions of selected sediment samples, the 1σ analytical error of the U^{K}_{37} SST estimates is ±0.2°C. AMS ^{14}C ages were determined on monospecific samples of *G. ruber* (white) and *G. sacculifer*, except for one date (510 cm in core 18287-3) where a mixed sample of *G. ruber* and *G. sacculifer* was used (*12*). The radiocarbon age determinations were carried out at the Tandetron AMS facility at the Leibniz Laboratory, following standard procedures (*30, 31*).
7. K. Stattegger *et al.*, Geol.-Paläont. Inst. Rep 86 (Univ. of Kiel, Kiel, Germany, 1997).
8. M. Kienast, unpublished data.
9. C. Pelejero, J. O. Grimalt, S. Heilig, M. Kienast, L. Wang, *Paleoceanography* **14**, 224 (1999).
10. D. Nürnberg, A. Müller, R. R. Schneider, *Paleoceanography* **15**, 124 (2000).
11. S. Steinke, M. Kienast, U. Pflaumann, M. Weinelt, K. Stattegger, *Quat. Res.*, in press.
12. Web table 1 is available at *Science* Online at www.sciencemag.org/cgi/content/full/291/5511/2132/DC1.
13. D. A. Meese *et al.*, *J. Geophys. Res.* **102**, 26411 (1997).
14. E. Bard, *Paleoceanography* **3**, 635 (1988).
15. L. Wang *et al.*, *Mar. Geol.* **156**, 245 (1999).
16. T. Hanebuth, K. Stattegger, P. M. Grootes, *Science* **288**, 1033 (2000).
17. D. M. Anderson, R. C. Thunell, *Quat. Sci. Rev.* **12**, 465 (1993).
18. The midpoint of the warming step in core 17940-2 occurs at 810 cm, bracketed between AMS ^{14}C ages of 13,490 ± 140 years at 792.5 cm and 14,360 +154/-152 years at 842.5 cm (*15*). Linear interpolation between these dates yields a calibrated age of 15,970 +284/-259 years (1σ range) for the midpoint of the warming.
19. O. Cayre, E. Bard, *Quat. Res.* **52**, 337 (1999).
20. M. Lyle, F. G. Prahl, M. A. Sparrow, *Nature* **355**, 812 (1992).
21. A. C. Mix, A. E. Morey, in *The South Atlantic: Present and Past Circulation*, G. Wefer, W. H. Berger, G. Siedler, D. J. Webb, Eds. (Springer-Verlag, Berlin, 1996), pp. 503–525.
22. H. Doose, F. G. Prahl, M. Lyle, *Paleoceanography* **12**, 615 (1997).
23. I. Cacho *et al.*, *Paleoceanography* **14**, 698 (1999).
24. E. Bard, F. Rostek, J. L. Turon, S. Gendreau, *Science* **289**, 1321 (2000).
25. S. S. Kienast, J. McKay, *Geophys. Res. Lett.*, in press.
26. A. L. Berger, *Quat. Res.* **9**, 139 (1987).
27. J. Villanueva, C. Pelejero, J. O. Grimalt, *J. Chromatogr.* **757**, 145 (1997).
28. C. Pelejero, J. O. Grimalt, *Geochim. Cosmochim. Acta* **61**, 4789 (1997).
29. P. J. Müller, G. Kirst, G. Ruhland, I. von Storch, A. Rosell–Mele, *Geochim. Cosmochim. Acta* **62**, 1757 (1998).
30. M.-J. Nadeau *et al.*, *Nucl. Instrum. Methods Phys. Res. B* **123**, 22 (1997).
31. M. Schleicher, P. M. Grootes, M.-J. Nadeau, A. Schoon, *Radiocarbon* **40**, 85 (1998).
32. M. Stuiver, P. M. Grootes, *Quat. Res.* **53**, 277 (2000).

33. The authors express their gratitude to P. M. Grootes, H. Erlenkeuser, and their lab teams at the Leibniz Laboratory in Kiel, Germany, for AMS ^{14}C dating and foraminiferal isotope analyses. We thank S. S. Kienast and C. Pelejero for invaluable assistance with the alkenone analyses. We are grateful to S. S. Kienast and T. F. Pedersen, as well as two anonymous referees, for their constructive comments on this article. Supported by research grants to S.E.C. [Natural Sciences and Engineering Research Council (NSERC), Canada] and K.S. [German Federal Ministry of Education and Research (BMBF), Germany], as well as by University of British Columbia Killam predoctoral (M.K.) and [German Academic Exchange Service (DAAD)] (S.S.) fellowships.

3 November 2000; accepted 16 February 2001